International Journal of Heat and Mass Transfer 51 (2008) 6317–6322

Contents lists available at ScienceDirect

International Journal of Heat and Mass Transfer

journal homepage: www.elsevier.com/locate/ijhmt

Technical Note

An analytical solution for the total heat transfer in the thin-film region of an evaporating meniscus

Hao Wang [a], Suresh V. Garimella [b,*], Jayathi Y. Murthy [b]

[a] Department of Energy and Resources Engineering, College of Engineering, Peking University, Beijing 100871, China
[b] Cooling Technologies Research Center, School of Mechanical Engineering, Purdue University, West Lafayette, IN 47907-2088, USA

ARTICLE INFO

Article history:
Received 4 October 2007
Received in revised form 7 June 2008
Available online 27 July 2008

Keywords:
Meniscus
Thin-film region
Disjoining pressure
Evaporation
Analytical solution

ABSTRACT

When a liquid wets a solid wall, the extended meniscus may be divided into three regions: a non-evaporating region where liquid is adsorbed on the wall; a thin-film region where effects of long-range molecular forces (disjoining pressure) are felt; and an intrinsic meniscus region where capillary forces dominate. Among these, the thin-film region is characterized by high heat transfer rates because its small thickness results in a very low conduction resistance. In this work, a simplified model based on the augmented Young–Laplace equation is developed and an analytical solution is obtained for the total heat transfer in the thin-film region. The results are consistent with previously published numerical solutions. The present work is valid for a much wider range of fluid thermal conductivity than a previous analytical solution by Schonberg and Wayner, which is only applicable for fluids with very low conductivity. Based on the analytical expression developed, the thin-film heat transfer is found to increase with increasing disjoining pressure, and to decrease with increasing liquid viscosity.

1. Introduction

When a liquid wets a solid wall in an ambient of air, the disjoining pressure has been defined as being equal to the difference between the pressure applied by the liquid film on the air and solid phases by which it is confined and the pressure in the bulk of the liquid film in a state of isothermal and isobaric equilibrium [1]. When the liquid film is thin enough, the liquid–gas and liquid–solid interfaces interfere with each other, giving rise to disjoining pressure. According to this definition, as a first approximation, the disjoining pressure is equal to the sum of contributions from the following components: a molecular component, dependent on the effect of molecular or dispersion forces; an ionic–electrostatic component, dependent on the overlapping of diffuse ionic atmospheres; an adsorption component, dependent on the overlapping of diffuse atmospheres of adsorbed molecules; a structural component; and finally, an electronic component, dependent on the overlapping of near-surface layers of liquid metals (like mercury), in which the wave functions of electrons are different from the bulk [1].

It has been decades since the concept of disjoining pressure was introduced in the science of colloids and surface phenomena. In the field of heat transfer, it has been studied because of its importance in the thin-film region. Deryagin et al. [2] demonstrated liquid pressure reduction in the thin-film region due to disjoining pressure. Potash and Wayner [3] concluded that the variation of disjoining pressure along the meniscus provides the necessary pressure gradient for liquid supply into the thin-film region. Wayner et al. [4] discussed the effects of disjoining pressure on liquid supply as well as its role in suppressing evaporation. As an extension of [4], Schonberg and Wayner [5] investigated the thin film by ignoring capillary pressure and developed an analytical solution for the maximum heat evaporated from the thin film; their analysis, however, was applicable only to insulating fluids.

Hallinan et al. [6] and DasGupta et al. [7] developed a fourth-order ordinary differential equation for solving the augmented Young–Laplace equation and obtained the thickness profile of the extended meniscus. The influence of superheat on the thin-film profile was discussed. Park et al. [8] proposed a mathematical model which included the vapor region and a slip boundary condition. It was concluded that the pressure gradient in the vapor region significantly affected the thin-film profile. Wee et al. [9] discussed evaporation in the thin-film region of a binary mixture. Recently, thin-film evaporation in a microchannel was studied [10]. The thin film was maintained throughout at a temperature below the saturation temperature corresponding to the imposed pressure, and the gas domain was assumed to consist of a mixture of air and vapor. The vapor diffusion in the gas domain was calculated to obtain the evaporation flux, and heat transfer results in the form of a local Nusselt number were reported. In the authors' previous work [11], a superheated meniscus was investigated using a

* Corresponding author. Tel.: +1 765 494 5621.
E-mail address: sureshg@purdue.edu (S.V. Garimella).

0017-9310/$ - see front matter © 2008 Elsevier Ltd. All rights reserved.
doi:10.1016/j.ijheatmasstransfer.2008.06.011

Nomenclature

A	dispersion constant (J)
H	height of channel (m)
h_{fg}	latent heat of evaporation (J/kg)
h_{lv}	evaporative heat transfer coefficient (W/m^{2}K)
k_l	liquid conductivity (W/mK)
m'	mass flow rate (kg/ms)
m''	interface net mass flux (kg/m^{2}s)
m''_{id}	ideal interface net mass flux (kg/m^{2}s)
M''	dimensionless interface mass flux
$\overline{M}$	molecular weight (kg/mol)
$\overline{R}$	universal gas constant (J/mol K)
P_c	capillary pressure
P_d	disjoining pressure (N/m^2)
P_l	liquid pressure (N/m^2)
ΔP_l	change of liquid pressure (N/m^2)
P_{sat}	saturation pressure (N/m^2)
P_v	vapor pressure (N/m^2)
P_{v_equ}	equilibrium pressure (N/m^2)
q	integrated heat transfer rate (W/m)
q_t	total heat transfer rate (W/m)
R	meniscus radius (m)
R^*	asymptotic intrinsic meniscus radius (m)
T	temperature (K)
u	velocity along x-axis (m/s)
V	molar volume (m^3/mol)
x	x-coordinate (m)
x_0	reference position defined in Eq. (19)
y	y-coordinate (m)

Greek symbols

δ	liquid layer thickness (m)
δ_0	non-evaporating region thickness (m)
η	dimensionless thickness
ν	kinematic viscosity (m^2/s)
μ	dynamic viscosity (Ns/m^2)
ρ_l	liquid density (kg/m^3)
ρ_v	vapor density (kg/m^3)
ξ	dimensionless position
λ	dimensionless group defined in Eq. (20)
σ	surface tension coefficient (N/m)
$\hat{\sigma}$	accommodation coefficient

Subscripts

c	condensation
e	evaporation
l	liquid
lv	liquid–vapor interface
sat	saturated
sum	sum
t	thin-film region
v	vapor

kinetic theory-based expression for mass transport across a liquid–vapor interface [12]; the boundary conditions for the film profile were discussed in detail, and the thin-film and the intrinsic-meniscus regions were distinguished based on the disjoining-pressure variation along the meniscus.

In the present work, an analytical solution is derived to more easily evaluate the total heat transfer in the entire thin-film region. The starting point is the model described in [11], referred to in this paper as the "full model," and its numerical solution. The full model is then simplified, making it possible to derive an analytical solution which follows. The analytical solution is compared to the numerical solution of the full model [11] and also to Schonberg and Wayner's numerical and analytical solutions [5].

2. Full model and numerical solution

The equations governing the thin-film profile have been extensively discussed in the literature [3–10] and are reviewed in the authors' previous work [11]. The problem under consideration is illustrated in Fig. 1. The pressure difference between vapor and liquid at the liquid–vapor interface is due both to the capillary and disjoining pressures, and is expressed using the augmented Young–Laplace equation [4]:

$$P_v = P_l + P_c + P_d \tag{1}$$

The disjoining pressure for a non-polar liquid is expressed as [4,5]

$$P_d = A/\delta^3 \tag{2}$$

where A is the dispersion constant and δ the film thickness. It is noted that in [5], the equation is $P_d = -A/\delta^3$; therefore, the sign of A in Eq. (2) is opposite to that used in [4,5]. The capillary pressure is the product of interfacial curvature K and surface tension coefficient σ

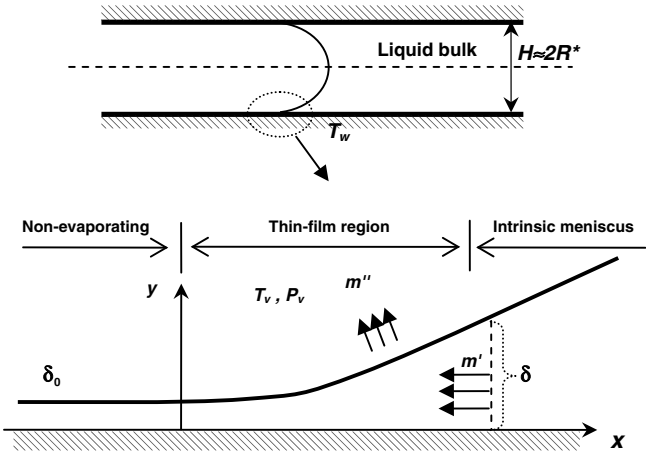

Fig. 1. Schematic diagram and coordinate system for an evaporating thin film in a channel.

$$P_c = \sigma K, \quad K = \delta''(1+\delta'^2)^{-1.5} \tag{3}$$

where δ' and δ'' are, respectively, the first and second derivatives of thickness with respect to length x.

Combining Eqs. (1)–(3) and differentiating with respect to x, the following third-order differential equation is obtained for the thin-film profile $\delta(x)$

$$\delta''' - \frac{3\delta'\delta''^2}{1+\delta'^2} + \frac{1}{\sigma}\left(\frac{dP_l}{dx} - \frac{3A}{\delta^4}\delta'\right)\left(1+\delta'^2\right)^{1.5} = 0 \tag{4}$$

assuming uniform P_v along the meniscus. In view of the very low Reynolds number and the large length-to-height ratio of the thin film, lubrication theory is employed to obtain the pressure gradient in Eq. (4). A no-slip boundary condition at the wall and a no-

Table 1
Properties of evaporating liquid [5] and operating conditions

Liquid	Octane
A (J)	3.18×10^{-21}
P_v (Pa)	1.5828×10^4
ρ_l (kg/m^3)	661.2
k_l (W/mK)	0.11
h_{fg} (kJ/kg)	339.8
T_w (K)	344
T_v (K)	343
$\hat{\sigma}$	1

shear boundary condition at the liquid–vapor interface are imposed. Under these assumptions, the liquid pressure gradient dP_l/dx may be related to the mass flow rate $m'(x)$. At steady state, the mass flow rate $m'(x)$ at a position x is equal to the integral of the net evaporative mass flux from the beginning of the film to the local position. The liquid pressure gradient may then be obtained as

$$\frac{dP_l}{dx} = \frac{3v}{\delta^3}\int_{-\infty}^{x} m''\,dx \tag{5}$$

Substituting the pressure gradient into Eq. (4) and further differentiating with respect to x, a fourth-order ordinary differential equation is obtained for the thin-film profile

$$\frac{d}{dx}\left(\left[\frac{\sigma\delta'''}{(1+\delta'^2)^{1.5}} - \frac{3\sigma\delta'\delta''^2}{(1+\delta'^2)^{2.5}} - \frac{3A\delta'}{\delta^4}\right]\frac{\delta^3}{3v}\right) = -m'' \tag{6}$$

In the authors' previous work [11], Eq. (6) was solved numerically. The particular system considered was the evaporation of a film of octane on a silicon substrate. The vapor domain was assumed to be saturated at T_v and P_v. The relevant properties are listed in Table 1. The dispersion constant A was assumed to be -3.18×10^{-21} J based on the data in [13], which considered octane on silicon with air at room temperature. The accommodation coefficient $\hat{\sigma}$ for the evaporation calculation was assumed to be unity for octane, a non-polar liquid.

Fig. 2 shows the variation of the different components of pressure along the film length when the superheat is 1 K. The thin-film region is identified as ending at a location when the disjoining pressure drops to 1/2000th of P_{d0}, which is the disjoining pressure in the non-evaporating region [11]. Based on this definition, it is seen in Fig. 2 that the length of the thin-film region is approximately 150 nm. The total heat transfer q_t from this thin-film region was calculated to be 0.139 W per unit depth. It was also found that the length of the thin-film region and q_t were insensitive to channel size when it was larger than a few micrometers. Details of the numerical solution are available in [11].

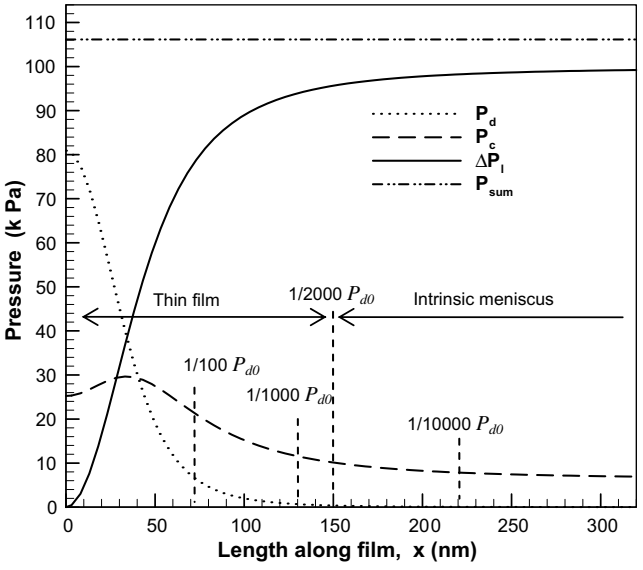

Fig. 2. Variation of the different pressure components along the length of the meniscus [11] (superheat 1 K, $R^* = 2500$ nm).

3. Analytical solution for total heat transfer from thin-film region

To derive an analytical solution for q_t, we will first simplify the governing equations. Two simplifications are made based on results of the full model in Section 2:

1. By definition, the thin-film region is the region supported by disjoining pressure. Disjoining pressure drops from the non-evaporating region to the intrinsic meniscus, which allows liquid to flow from the bulk into the film to compensate for evaporation. It is supposed that q_t can be determined mostly from the drop in disjoining pressure. The governing equation may then be simplified by ignoring capillary pressure and setting $\sigma = 0$ on the left side of Eq. (6)

$$\frac{d}{dx}\left\{-\frac{A}{\delta v}\delta'\right\} = -m'' \tag{7}$$

2. In [11] the evaporation mass flux m'' was calculated using the kinetic theory-based expression developed by Schrage [12]. In the present work, m'' is calculated using a simplified evaporation model proposed by Wayner et al. [4]

$$m'' = a(T_{lv} - T_v) - b(P_d + P_c) \tag{8a}$$

where

$$a = C\left(\frac{\overline{M}}{2\pi\overline{R}T_{lv}}\right)^{1/2}\frac{P_v\overline{M}h_{fg}}{\overline{R}T_vT_{lv}}, \quad b = C\left(\frac{\overline{M}}{2\pi\overline{R}T_{lv}}\right)^{1/2}\frac{V_lP_v}{RT_{lv}} \tag{8b}$$

Eq. (8) is obtained from Schrage's original expression by using an extended Clapeyron equation [4] and the approximations $T_{lv} \approx T_v$ and $P_{v\_equ} \approx P_v$. The second group on the right side of Eq. (8a) represents the suppression of evaporation by disjoining and capillary pressure. The suppression is significant only within the thinnest part of the thin-film region, and neglecting it does not significantly influence q_t. Assuming the suppression component to be negligible, we may write

$$m'' = a(T_{lv} - T_v) \tag{9}$$

The evaporation heat transfer is $q'' = m''h_{fg}$ and the evaporative heat transfer coefficient is therefore

$$h_{lv} = ah_{fg} \tag{10}$$

Now, the conduction heat transferred through the liquid film should equal the evaporative heat flux. Using this, an expression for m'' in terms of the wall temperature T_w can finally be obtained as

$$m'' = \frac{1}{h_{fg}}\frac{h_{lv}k_l(T_w - T_v)}{k_l + h_{lv}\delta} \tag{11}$$

Combining Eqs. (11) and (7), the simplified governing equation for the thin-film profile may be rewritten as

$$\frac{d}{dx}\left(\frac{A}{\delta v}\left(\frac{d\delta}{dx}\right)\right) = \frac{1}{h_{fg}}\frac{h_{lv}k_l(T_w - T_v)}{k_l + h_{lv}\delta} \tag{12}$$

A non-dimensionalization similar to that in Schonberg and Wayner [5] may be carried out. A dimensionless thickness is first defined as

$$\eta = \frac{\delta}{\delta_0} \tag{13}$$

in which δ_0 is the thickness of the non-evaporating region. Setting $m'' = 0$ in Eq. (8a) gives

$$\delta_0 = \left(\frac{b}{a}\frac{A}{T_w - T_v}\right)^{1/3} \tag{14}$$

A dimensionless position

$$\xi = \frac{x}{x_0} \tag{15}$$

and a dimensionless evaporative mass flux

$$M'' = \frac{m''}{m''_{id}} \tag{16}$$

are also defined in which m''_{id} is the ideal flux in the absence of a pressure effect, i.e., with $b = 0$ in Eq. (8a)

$$m''_{id} = a(T_w - T_v) \tag{17}$$

With these definitions, the governing equation (12) becomes

$$\frac{A}{x_0^2 \nu m''_{id}}\frac{d}{d\xi}\left(\frac{1}{\eta}\left(\frac{d\eta}{d\xi}\right)\right) = \frac{1}{1+\frac{ah_{fg}\delta_0\eta}{k_l}} \tag{18}$$

Defining

$$x_0 \equiv \sqrt{\frac{A}{\nu m''_{id}}} \tag{19}$$

and a dimensionless group

$$\lambda \equiv \frac{ah_{fg}\delta_0\eta}{k_l} \tag{20}$$

the non-dimensionalized governing equation takes the form

$$\frac{d}{d\xi}\left(\frac{1}{\eta}\left(\frac{d\eta}{d\xi}\right)\right) = \frac{1}{1+\lambda\eta} \tag{21}$$

Comparing this equation to the governing equation derived in Schonberg and Wayner [5]

$$\frac{d}{d\xi}\left(\frac{1}{\eta}\left(\frac{d\eta}{d\xi}\right)\right) = \frac{1}{1+\lambda\eta}\left(1-\frac{1}{\eta^3}\right) \tag{22}$$

it is seen that the last term on the right is neglected, i.e.

$$1 - \frac{1}{\eta^3} \approx 1 \tag{23}$$

This approximation has its origin in the neglect of the suppression of evaporation by disjoining and capillary pressure, as explained with Eq. (9). When the film thickness is very close to the non-evaporating thickness δ_0, the disjoining pressure is very large and the evaporation is suppressed strongly. Under such conditions, $\delta/\delta_0 \approx 1$ and $(1 - 1/\eta^3) \approx 0$, and the approximation is not appropriate. However, it is noted that $1/\eta^3$ decreases towards zero very quickly as the thickness grows, for example, $(1 - 1/\eta^3) = 0.962$ when $\eta = 3$, and is equal to 0.992 when $\eta = 5$. Since the goal of the present work is to obtain a solution for the total heat transfer in the thin-film region, the heat transfer from the part of the film very close to the non-evaporating region may be neglected compared to the total heat transfer q_t. As seen in Section 4.2, this approximation induces negligible error in the q_t calculation.

Solving the governing equation (12), the slope of the film profile is obtained as

$$\frac{d\delta}{dx} = \delta\sqrt{2C_1\left(\ln\frac{\delta}{\delta_0}\frac{1+C_2\delta_0}{1+C_2\delta}\right)} \quad \text{with } C_1 = \frac{\nu}{A}\frac{h_{lv}(T_w - T_v)}{h_{fg}}C_2 = \frac{h_{lv}}{k_l} \tag{24}$$

On the other hand, the mass flow rate through the cross-section at a position x, $m'(x)$, may be obtained from lubrication theory as [5]

$$m'(x) = \frac{A}{\delta\nu}\left(\frac{d\delta}{dx}\right) \tag{25}$$

As illustrated in Fig. 1, it is equal to the integral of the evaporative mass flux from the beginning of the film to position x. Therefore, the total heat dissipated from the beginning of the film to position x is

$$q(x) = m'(x)h_{fg} \tag{26}$$

Combining Eqs. (24) and (25) with Eq. (26) yields

$$q = m'h_{fg} = \sqrt{\frac{2Ah_{fg}h_{lv}(T_w - T_v)}{\nu}\ln\left(\frac{\delta}{\delta_0}\frac{1+C_2\delta_0}{1+C_2\delta}\right)} \tag{27}$$

To obtain the total heat transfer from the entire thin-film region, the thickness δ is set to infinity in the above equation, yielding

$$q_t = \sqrt{\frac{2Ah_{fg}h_{lv}(T_w - T_v)}{\nu}\ln\left(\frac{k_l}{h_{lv}\delta_0} + 1\right)} \tag{28}$$

It can be seen from this expression that thin-film heat transfer increases with disjoining pressure and decreases with liquid viscosity. Disjoining pressure supports the thin film, and as pointed out in the literature [3–11], its reduction along the film length allows liquid to flow from the bulk into the film to compensate for evaporation. Higher liquid viscosity creates greater resistance to liquid flow and reduces this compensatory flow, thereby reducing q_t.

4. Results and discussion

4.1. Comparison of analytical solution and full model

A comparison between the analytical solution, i.e., Eq. (28), and the numerical solution of the full model in [11] is shown in Fig. 3. It is seen from Fig. 3a that the analytical solution agrees well with the full model. Only when the wall superheat is very small (<0.1 K) does the analytical solution overestimate q_t, as seen in Fig. 3b. It may be noted that the simplified evaporation equations, Eqs. (9) and (10), neglect the suppression of evaporation by P_d and P_c, as described in Section 3. The suppression is more significant for lower wall superheat or lower T_{lv}. If the suppression is taken into account, h_{lv} should be

$$h_{lv} = h_{fg}\left[a - b(P_d + P_c)\frac{1}{(T_{lv} - T_v)}\right] \tag{29}$$

It is seen that a smaller $T_{lv} - T_v$ amplifies the second term in the brackets and depresses h_{lv}.

The error engendered by neglecting the suppression can be reduced by the following improvement to the model. Along the meniscus, $P_d + P_c$ decreases monotonically to $P_c^* = \sigma/R^*$, which is the capillary pressure in the intrinsic meniscus. That is, the minimum value of $(P_d + P_c)$ is P_c^*. Using P_c^* in Eq. (29), an improved h_{lv} may be obtained as

$$h_{lv} = h_{fg}\left[a - b\frac{\sigma}{R^*}\frac{1}{(T_w - T_v)}\right] \tag{30}$$

With the suppression component added to the analytical solution, it is seen in Fig. 3b that the improved h_{lv} can effectively reduce the overestimation of q_t at low superheats.

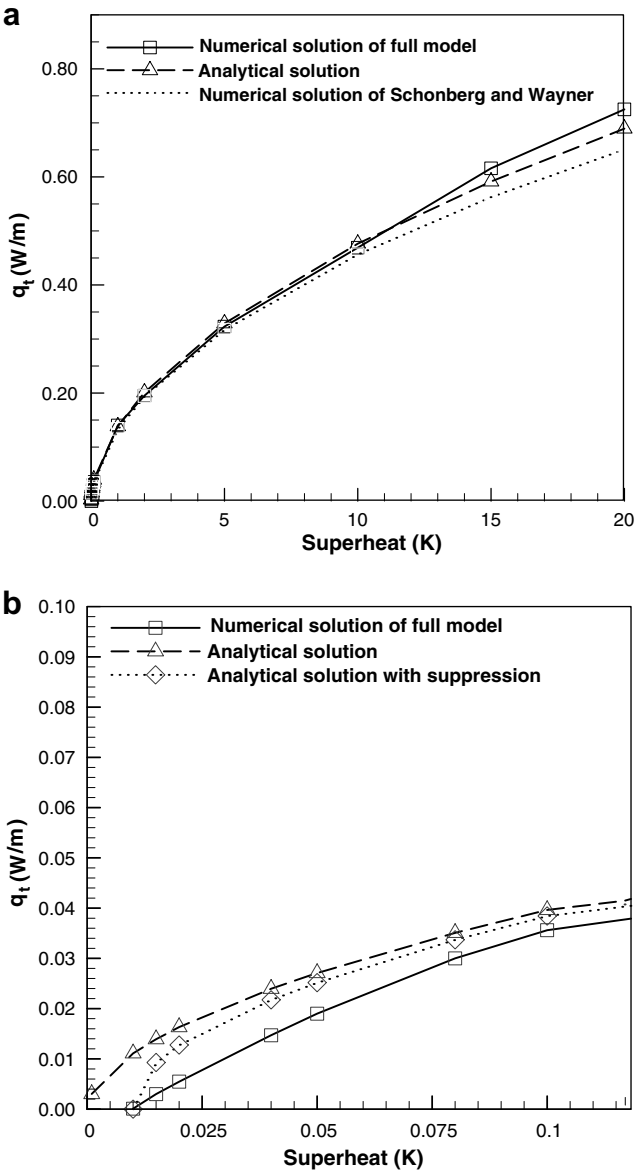

Fig. 3. Comparison of q_t from the present analytical solution with the numerical solution of the full model from [11]. These solutions are also compared to (a) the numerical solution of Schonberg and Wayner [5], and (b) the present analytical solution modified to account for the suppression by disjoining pressure and capillary pressure, shown at low wall superheats.

We note here that although the analytical solution in Eq. (28) is found to be appropriate for computing the total heat transfer from the thin-film region, this does not imply that the capillary pressure may be neglected in calculating the film profile. In fact, capillary pressure plays an important role in shaping the film profile, including in the thin-film region [11].

4.2. Comparison to numerical and analytical solutions of Schonberg and Wayner [5]

By neglecting capillary pressure, Schonberg and Wayner [5] derived Eq. (22) for the thin-film profile and solved it for q_t. Although both numerical and analytical solutions were obtained for Eq. (22), the analytical solution is valid only when the liquid conductivity is very small, i.e., for an insulating liquid.

Fig. 3 shows a comparison of the numerical solution of [5] with the analytical solution (without the suppression component) developed in the present work. Very good agreement between

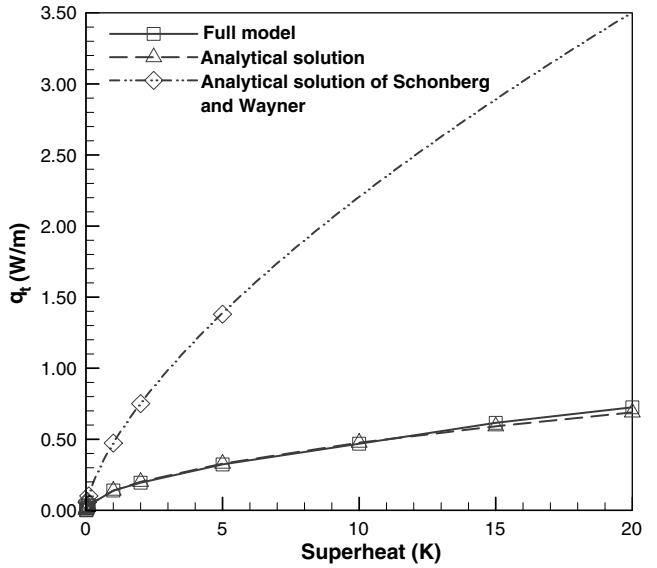

Fig. 4. Comparison of the analytical solution (without the suppression component) from the present work with the analytical solution of Schonberg and Wayner [5] when liquid conductivity $k_l = 0.11$ W/mK (small λ).

the two sets of results is observed. The values from the present analytical solution are a little higher than the numerical solution, which is a result of the lack of the inclusion of suppression of evaporation in the present model.

For the extreme case of large $\lambda = ah_{fg}\delta_0/k_l$, Schonberg and Wayner [5] also obtained the following analytical solution:

$$q_t = \sqrt{\frac{3}{2}} A^{1/3} \left(\frac{h_{fg}k_l}{\nu}\right)^{1/2} \left(\frac{a}{b}\right)^{1/6} (T_w - T_v)^{2/3} \tag{31}$$

As shown in Fig. 4, three curves are plotted: the analytical solution from the present work, the analytical solution of [5], and the numerical solution from the full model [11]. It is apparent that the analytical solution in the present work is consistent with the full model, while Schonberg and Wayner's analytical solution deviates significantly. The reason is that the analytical solution in

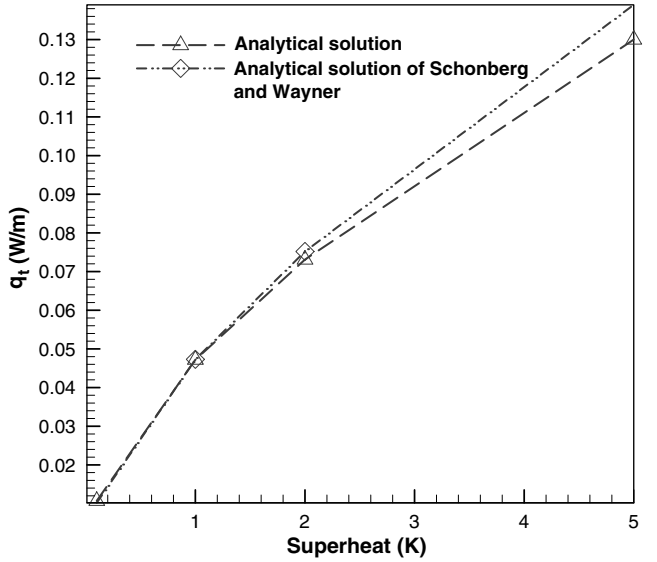

Fig. 5. Comparison of the present analytical solution (without the suppression component) with that of Schonberg and Wayner [5] when liquid conductivity $k_l = 1.1 \times 10^{-3}$ W/mK (large λ).

Eq. (31) was derived under the condition that the term $\lambda = ah_{fg}\delta_0/k_l$ is large, as addressed in [5]. Since δ_0 is of the order of nanometers and ah_{fg} is of the order of 10^6 W/m^{2}K, $ah_{fg}\delta_0/k_l > 1$ implies conductivity $k_l < 10^{-3}$ W/mK. For octane, the value of k_l is equal to 0.11 W/mK, and not small enough for Eq. (31) to apply.

If the liquid conductivity is very small, for example, $k_l = 1.1 \times 10^{-3}$ W/mK, Eq. (31) would produce much less error, and the two analytical solutions agree more closely, as seen in Fig. 5.

5. Conclusions

A simplified model neglecting capillary pressure is developed for the thin-film region of an evaporating meniscus, and an analytical solution is obtained for the total heat transfer in the thin-film region. The results agree well with the numerical solution for the full model described in [11] in which the thin-film region is identified as ending at a location when the disjoining pressure drops to 1/2000th of P_{d0}, the disjoining pressure in the non-evaporating region. The results also agree with the analytical solution provided by Schonberg and Wayner [5] when the fluid conductivity is very small, since their solution is applicable only to insulating liquids. Thin-film heat transfer is seen to increase with an increase in disjoining pressure, and decrease with increasing liquid viscosity.

Acknowledgements

The authors acknowledge financial support for this work from members of the Cooling Technologies Research Center, a National Science Foundation Industry/University Cooperative Research Center at Purdue University.

References

[1] B.V. Derjaguin, Modern state of the investigation of long-range surface forces, Langmuir 3 (5) (1987) 601–606.
[2] B.V. Deryagin, S.V. Nerpin, N.V. Churayev, Effect of film heat transfer upon evaporation of liquids from capillaries, Bull. R. I. L. E. M. 29 (1965) 93–98.
[3] M. Potash Jr., P.C. Wayner Jr., Evaporation from a two-dimensional extended meniscus, Int. J. Heat Mass Transfer 15 (1972) 1851–1863.
[4] P.C. Wayner Jr., Y.K. Kao, L.V. LaCroix, The interline heat transfer coefficient of an evaporating wetting film, Int. J. Heat Mass Transfer 19 (1976) 487–492.
[5] J.A. Schonberg, P.C. Wayner Jr., Analytical solution for the integral contact line evaporative heat sink, J. Thermophys. Heat Transfer 6 (1992) 128–134.
[6] K.P. Hallinan, H.C. Chebaro, S.J. Kim, W.S. Chang, Evaporation from an extended meniscus for nonisothermal interfacial conditions, J. Thermophys. Heat Transfer 8 (1994) 709–716.
[7] S. DasGupta, J.A. Schonberg, P.C. Wayner Jr., Investigation of an evaporating extended meniscus based on the augmented Young–Laplace Equation, J. Heat Transfer 115 (1993) 201–208.
[8] K. Park, K. Noh, K. Lee, Transport phenomena in the thin-film region of a microchannel, Int. J. Heat Mass Transfer 46 (2003) 2381–2388.
[9] S. Wee, K.D. Kihm, D.M. Pratt, J.S. Allen, Microscale heat and mass transport of evaporating thin film of binary mixture, J. Thermophys. Heat Transfer 20 (2006) 320–327.
[10] C. Chakraborty, S.K. Som, Heat transfer in an evaporating thin liquid film moving slowly along the walls of an inclined microchannel, Int. J. Heat Mass Transfer 48 (2005) 2801–2805.
[11] H. Wang, S.V. Garimella, J.Y. Murthy, Characteristics of an evaporating thin film in a microchannel, Int. J. Heat Mass Transfer 50 (2007) 163–172.
[12] R.W. Schrage, A Theoretical Study of Interface Mass Transfer, Columbia University Press, New York, 1953.
[13] J.G. Truong, P.C. Wayner Jr., Effect of capillary and van der Waals dispersion force on the equilibrium profile of a wetting fluid: theory and experiment, J. Chem. Phys. 87 (1987) 4180–4188.